Microfluid Nanofluid (2014) 17:317–324
DOI 10.1007/s10404-013-1308-4

RESEARCH PAPER

Enhancing nanoparticle deposition using actuated synthetic cilia

Matthew Ballard · Zachary Grant Mills · Samuel Beckworth · Alexander Alexeev

Received: 2 August 2013 / Accepted: 10 December 2013 / Published online: 19 December 2013

Abstract We use computational modeling to probe the utility of actuated synthetic cilia lining walls of a microfluidic channel for enhancing the deposition of nanoparticles dispersed in a viscous fluid filling the channel. We demonstrate that elastic cilia actuated by a sinusoidal force applied to their free ends generate circulatory secondary flows facilitating nanoparticle transport. We identify optimal operational conditions in which the effect of cilia beating on particle deposition is maximized. Our simulations also reveal that cilia transition to a three-dimensional beating pattern when the actuation force exceeds a critical value. This transition is associated with buckling instability experienced by elastic cilia. Our findings guide the optimal design of ciliated microfluidic systems for uses such as deposition of particulates onto sensory surfaces and microfluidic mixing.

Keywords Synthetic cilia · Microfluidics · Nanoparticle deposition

1 Introduction

A variety of biological organisms utilize beating cilia to create flows in the surrounding fluid which help them to transport, capture, and absorb nutrients, as well as to expel foreign objects (Riisgard and Larsen 2001; Sleigh 1989). Cilia are tiny elastic filaments that are a few micrometers in length. Due to their small size, cilia operate at a low-Reynolds-number environment, in which the fluid motion is dominated by the fluid viscosity, whereas the inertial effects can be safely neglected. In this situation, a net fluid flow arises only when cilia perform a non-reciprocal, time-irreversible beating (Purcell 1977). Cilium elasticity combined with an asymmetric stroke (Satir and Christensen 2007; Wiggins et al. 1998; Brennen and Winet 1977) plays a critical role in generating required motion leading to efficient mass transport in a highly viscous fluidic environment.

The ability of biological cilia to regulate microscale transport processes has motivated researchers to design different types of biomimetic synthetic cilia (Pokroy et al. 2009; Wang et al. 2009; Tripathi et al. 2013; Vilfan et al. 2010; Timonen et al. 2010; Dayal et al. 2012; Malvadkar et al. 2010; Masoud and Alexeev 2011b). Such actuated and passive artificial cilia could be useful to enhance microscale transport processes in microfluidic devices (Den Toonder and Onck 2013b; Masoud and Alexeev 2011a; Semmler and Alexeev 2011; Shields et al. 2010). Researchers have designed and built synthetic elastic filaments that are actuated by various external stimuli. Evans et al. (2007) created high-aspect-ratio cantilevered synthetic cilia made of a PDMS–ferrofluid composite material and showed that they could be actuated using an external magnetic field. Oh et al. (2009) fabricated PDMS cilia and used a piezo-actuator to cause them to resonate in water. They demonstrated rapid fluid mixing performed by their synthetic cilia (Oh et al. 2010). Babataheri et al. (2011) coated a microtube with a carpet of flexible artificial cilia fabricated from superparamagnetic colloidal particles linked together with polyacrylic acid and generated a small net fluid flow in the tube by actuating the cilia with a time-varying magnetic field. Khaderi et al. (2011) actuated magnetic artificial cilia with a rotating permanent magnetic field so as to create metachronal-type waves and pump fluid through a microchannel. Keißner and Brücker (2012)

M. Ballard · Z. G. Mills · S. Beckworth · A. Alexeev (✉)
George W. Woodruff School of Mechanical Engineering, Georgia Institute of Technology, Atlanta, GA 30332, USA
e-mail: alexander.alexeev@me.gatech.edu

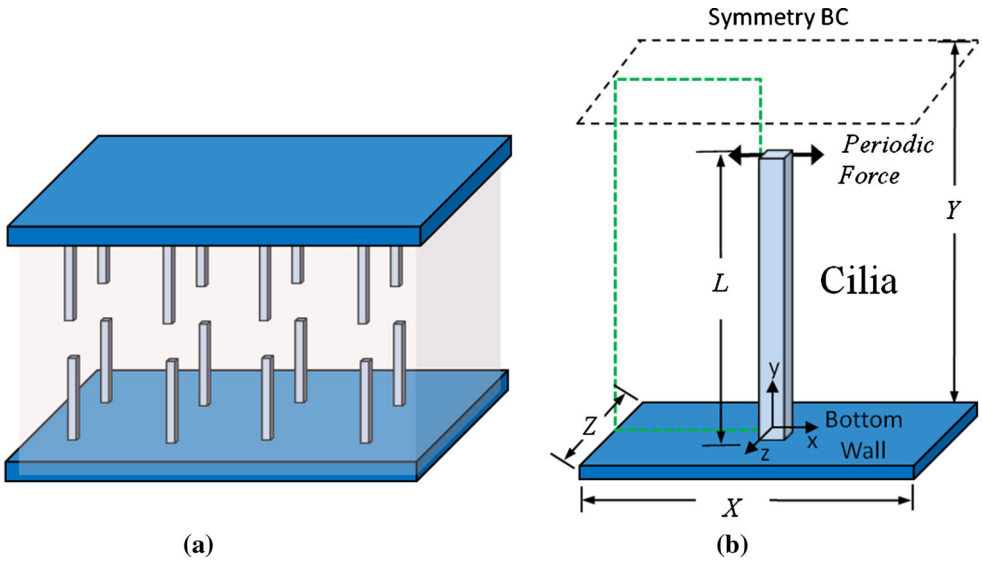

Fig. 1 **a** Schematic of a fluid-filled microchannel with periodic arrays of cilia on the top and bottom walls. **b** Periodic simulation domain, consisting of a single elastic cilium actuated by a periodic force applied horizontally at its tip. The *dotted line* shows the contour of a flow field plotted in Fig. 5

used PDMS cilia embedded into a thin membrane, and actuated by a ball-chain moved underneath the membrane, to induce fluid pumping in a microfluidic channel. Thus, it has been demonstrated that synthetic cilia can be fabricated and actuated and can indeed manipulate fluid in microfluidic systems.

Herein, we examine the ability of oscillating synthetic cilia to enhance the deposition of nanoparticles onto ciliated walls. To this end, we employ three-dimensional numerical simulations to investigate the deposition of nanoparticles dispersed in the viscous fluid in a microchannel with walls decorated by periodic arrays of oscillating synthetic cilia. We probe how system parameters including particle diffusivity, cilia oscillation frequency, actuation force amplitude, and cilia coverage density affect nanoparticle deposition at a low Reynolds number. We investigate the parameter space by systematically varying the parameters under investigation and determine the conditions at which the oscillating cilia are most effective in enhancing the deposition of nanoparticles.

2 Methodology

The system that we simulate consists of a microchannel filled with a viscous fluid. The top and bottom walls of the microchannel are decorated with arrays of elastic cilia (Fig. 1a), each with an aspect ratio of 10. The cilia are driven by a sinusoidal horizontal force applied at the cilia tips, causing them to periodically oscillate from their vertical equilibrium position.

In our study, we take the simulation domain to be the volume encompassing a single cilium (Fig. 1b) and apply periodic boundary conditions in the x- and z- (horizontal) directions, allowing for simulation of a microchannel with cilia arrays periodic in the horizontal directions. A symmetry boundary condition is applied at the top of the computational domain, representing a vertically symmetric microchannel with cilia on its top and bottom walls. To examine the effect of oscillating cilia on nanoparticle deposition, we introduce diffusive inertialess point particles that are initially uniformly distributed in the fluid. We track the evolution of the tracer particles and probe their deposition on the channel walls for cilia actuated with different frequencies and amplitudes.

In order to simulate our ciliated microchannel, we utilize a hybrid LBM/LSM method (Alexeev et al. 2005; Mills et al. 2013) that combines the lattice Boltzmann model (LBM) with a lattice spring model (LSM) to model the dynamic interactions between the viscous fluid and the elastic cilia. Additionally, this fluid–structure interaction model is coupled with a Brownian dynamics (BD) model to simulate nanoparticles within the system (Verberg et al. 2006).

The fluid dynamics is modeled using LBM, which is an efficient solver of incompressible viscous flows (Succi 2001; Ladd and Verberg 2001). LBM is particularly useful for flows in complex geometries, such as in microfluidic channels with walls covered by oscillating cilia. The LBM algorithm consists of two steps: a streaming step, in which fluid "particles" move along a space-fixed lattice to neighboring lattice nodes, and a collision step, in which the fluid "particles" collide at the nodes. These fluid "particles" represent mesoscopic amounts of the fluid and are described by a distribution function, $f_i(\mathbf{r}, t)$, which gives the mass density of fluid propagating in the direction i with velocity c_i at the lattice node $\mathbf{r}$ and time t. The hydrodynamic fields of the system are obtained by taking the moments of the distribution function, i.e., the mass density $\rho = \sum_i f_i$, the momentum $\mathbf{j} = \rho\mathbf{u} = \sum_i \mathbf{c}_i f_i$, where $\mathbf{u}$ is the local fluid velocity, and the stresses $\Pi = \sum_i \mathbf{c}_i \mathbf{c}_i f_i$. The

time evolution of the distribution function is governed by the discretized Boltzmann equation (Succi 2001). We use a D3Q19 lattice, which simulates a three-dimensional system using 19 particle-distribution functions at each node (Ladd and Verberg 2001). The height of the computational domain is set to be equal to 50 LBM units, and the lateral extent of the domain is varied in order to alter the coverage density of the cilia.

We simulate the dynamics of the elastic cilia using a LSM, which models the elastic solids as a system of uniformly distributed mass points (nodes) connected by harmonic springs (Buxton et al. 2001). A cilium is constructed from $4 \times 4 \times 32$ nodes arranged on a square lattice in which harmonic springs connect the nearest and next-nearest nodes (Ghosh et al. 2010; Alexeev et al. 2008). Two lower rows of nodes are fixed in space in order to impose a clamped boundary condition at the point of elastic cilium attachment to the wall. The equilibrium spacing between LSM nodes is equal to 4/3 LBM units. The cilia are arranged in a rectangular pattern with spacing δx and δz in the x and z directions, respectively (Fig. 1). In our simulations, we set $\delta z = \delta x/2$. We integrate Newton's equation of motion using the velocity Verlet algorithm to update the system dynamics at each time step (Tuckerman et al. 1992).

In our LBM/LSM simulations, the cilia and fluid interact through appropriate boundary conditions (Alexeev et al. 2005, 2006). Velocities of lattice spring nodes at the solid–fluid interface are transmitted to the surrounding fluids through a modified bounce-back rule (Bouzidi et al. 2001) that transfers momentum to the LBM distribution functions crossing the interface. LSM nodes on the boundary experience forces from the fluid pressure and viscous stresses calculated using the momentum exchange in the LBM fluid.

We model the movement of the nanoparticles in the fluid filling the microchannel using a BD method (Verberg et al. 2006, 2007). Particle trajectories are governed by the stochastic differential equation:

$$d\mathbf{r}(t) = \mathbf{u}(\mathbf{r}, t)dt + \sqrt{2D_0}d\mathbf{W}(t), \tag{1}$$

where $\mathbf{r}(t)$ is the particle location. The first term on the right represents the advection of particles due to the local fluid velocity $\mathbf{u}(\mathbf{r}, t)$, and the second term on the right describes the contribution of Brownian diffusion, where $D_0 = k_B T/6\pi\mu a$ is the diffusion coefficient of the particle in the fluid and $d\mathbf{W}(t)$ is the differential of a Wiener process with unit variance. Here, k_B is Boltzmann's constant, T is the absolute temperature, μ is the dynamic viscosity, and a is the nanoparticle radius. A discretized form of Eq. (1) is given by

$$\mathbf{r}(t + \Delta t) = \mathbf{r}(t) + \mathbf{u}[\mathbf{r}(t)]\Delta t + \sqrt{2D_0}\Delta\mathbf{W}(t) \tag{2}$$

where $\Delta\mathbf{W}$ is a random number sampled from a truncated Gaussian distribution with unit variance and is obtained using the Ziggurat method (Marsaglia and Tsang 2000). The local fluid velocity at the particle position is determined through linear interpolation of the fluid velocity at neighboring LBM nodes. In our simulations, we neglect the influence of nanoparticles on the fluid flow, as well as any interactions between nanoparticles, including their agglomeration in the flow. Furthermore, we neglect the momentum exchange between nanoparticles and oscillating cilia due to their collisions. These assumptions are relevant to relatively dilute suspensions with particle sizes much smaller than those of cilia.

In the simulations reported here, we use 10^4 particles. We assume that the cilia surface is perfectly reflective of the particles. In this case, the particles do not deposit on the cilia. To impose this condition, we reflect the particles off of the cilia by reversing the component of the particle velocity that is normal to the cilia surface. At the boundaries of the simulation domain, we apply a reflective boundary at the top of the domain and periodic boundary conditions in the horizontal directions (Fig. 1). At the bottom of the domain representing the bottom microchannel wall, any particle that crosses the boundary is assumed to be deposited, thereby simulating perfectly adsorptive walls. This assumption is valid in the situations when the number of adsorption sites is much larger than the amount of deposited nanoparticles, and/or nanoparticles can bind to each other forming continuous deposit layers. We track nanoparticle deposition and calculate the fraction of particles deposited on the microchannel walls in the course of the simulations to assess the effect of beating cilia on this process.

We characterize the system using several dimensionless parameters. The Schmidt number, $Sc = \nu/D_0$, gives the relative importance of momentum diffusion to particle diffusion in mass transport within the system. Here, ν is the kinematic viscosity of the fluid. The sperm number, $Sp = L(\zeta\omega/K)^{0.25}$, shows the ratio of viscous to elastic forces on the oscillating cilia and defines the bending pattern of the cilia. Here, L is the cilia length, ζ is the lateral drag coefficient of the cilia (defined here as $\zeta = 4\pi\rho\nu$), ω is the driving force oscillation frequency, and K is the bending rigidity of the cilia. The dimensionless force, $A = FL^2/3K$, gives the amplitude of the oscillatory force applied at the cilia tips scaled by cilia bending elasticity, where F is the amplitude of the oscillatory force driving the cilia.

We vary Sc, Sp, A, and δx to investigate the effects of particle diffusivity, cilia oscillation pattern, driving force amplitude, and cilia coverage density, respectively, on the ability of beating cilia to enhance deposition of nanoparticles on the walls of a microfluidic channel.

3 Results and discussion

In the absence of fluid flow, the deposition of nanoscopic particles is controlled by diffusion. If the particles in the fluid are taken to be a dilute liquid solution at constant temperature and pressure with no reactions and zero fluid velocity, the problem of deposition of nanoparticles from a quiescent fluid onto microchannel walls can be solved analytically by integrating the diffusion equation (Bird et al. 2002). The resulting analytical solution for the fraction of particles deposited on the microchannel walls, denoted by P, is given by

$$P = 1 - \frac{2}{\pi^2}\sum_{n=1}^{\infty}\frac{(1-(-1)^n)^2}{n^2}e^{(-n^2 t/\tau)}, \quad (3)$$

where $\tau \equiv H^2/D\pi^2$ is the diffusion timescale. The equation is obtained subject to boundary conditions of zero concentration at the channel walls (perfectly adsorptive walls) and an initial condition of a uniform concentration throughout the channel at time $t = 0$.

Figure 2a shows that the amount of deposited particles steadily increases with time. This figure also compares the theoretical predictions with the results of our computational model for the case of a microchannel without cilia. The results of simulations match closely with the analytical solution, indicating that our computational model correctly predicts diffusive transport and particle deposition in a microchannel.

When we introduce elastic cilia that are driven by a horizontally oscillating force, the deposition rate increases. Figure 2b shows a plot of P over time for both the case of oscillating cilia (solid line) and the case with no cilia (dashed line). The amount of deposited particles increases more quickly when the fluid is agitated by oscillating cilia, indicating that beating cilia enhance nanoparticle deposition by creating convective fluid flows.

In order to quantify the enhancement of deposition, we introduce a deposition enhancement factor $E_P = t_D/t_C$ where t_D is the time required to reach the desired deposition P without cilia and t_C is the time required to reach the same P with oscillating cilia. For the case shown in Fig. 2b, the deposition enhancement for 90 % deposition, denoted by $E_{0.9}$, was found to be 1.86. This means that 90 % of particles will be deposited almost two times faster using oscillating cilia as compared with the deposition in a plain channel.

The value of E depends upon P, as shown in the plots of E versus P for varying Sp and A given in Fig. 3a and b, respectively. For relatively short times $t \ll \tau$, deposition is limited to those nanoparticles that are located in the vicinity of the walls, in which case enhancement due to oscillating cilia is relatively weak. However, as the deposited P increases, E also increases. This can be explained by considering that the initial concentration of particles throughout the channel is uniform and particles located close to the walls can deposit fast due to molecular diffusion. As more particles deposit on the channel walls, the concentration of particles near the walls is reduced as compared with the center of the channel. This causes the deposition rate to slow as P increases (Fig. 2). If beating cilia are used to agitate the fluid, then the fluid from the center of the channel, which contains a higher concentration of particles, is brought closer to the walls, increasing the amount of particles that are near the walls, thereby facilitating their deposition. Thus, the influence of beating cilia on deposition increases with time as the concentration of particles in the channel drops.

We find that E increases monotonically for different values of Sp, as shown in Fig. 3a. Among three values of Sp shown in this figure, $Sp = 3$ yields a consistently larger E than somewhat larger and smaller values of Sp, indicating a non-trivial dependence of E on Sp. We also find that an increase in amplitude can enhance the deposition as indicated by increasing E in Fig. 3b. Below, we examine the dependence of E on Sp and A in more detail.

We first investigate the effect of Sp on the deposition of nanoparticles in a ciliated microchannel. As seen in Fig. 4, the dependence of E on Sp is non-monotonic, with two maxima at around $Sp = 3$ and $Sp = 5$, respectively. The maximum at $Sp = 3$ is significantly larger than at $Sp = 5$ and, therefore, characterizes the beating regime that is optimal for enhancing particle deposition. We find a

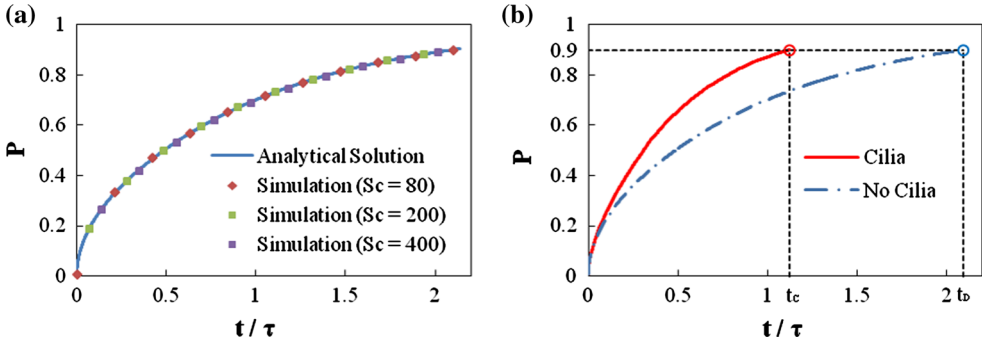

Fig. 2 **a** Diffusive deposition of nanoparticles in a microchannel without cilia. **b** Deposition of nanoparticles $Sc = 4{,}000$ on microchannel walls without cilia and with cilia beating at $Sp = 3$, $\delta x/L = 1$, and $A = 1$. The time required to achieve 90 % deposition is shown for each case and is denoted by t_D and t_C, respectively

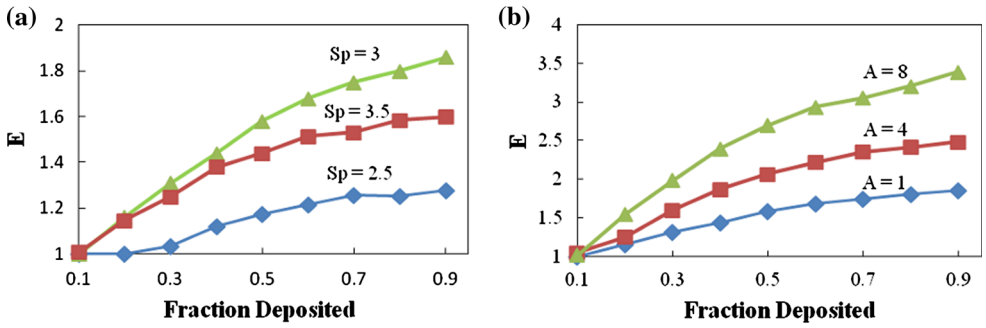

Fig. 3 Deposition enhancement E in ciliated microchannels with $\delta x/L = 1$ for nanoparticles with $Sc = 4{,}000$. **a** Cilia beating with different Sp and $A = 1$. **b** Cilia beating with different A and $Sp = 3$

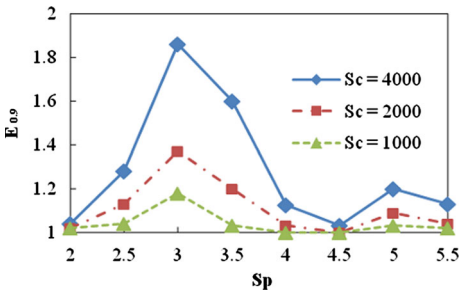

Fig. 4 Dependence of E at 90 % deposition on cilia sperm number Sp. The force amplitude is $A = 1$, and cilia separation is $\delta x/L = 1$

similar dependence of E on Sp for different values of Sc. Our simulations show that the enhancement is more significant for larger Sc. Because Sc relates the effects of fluid convection on mass transport to that of diffusion, an enhancement for larger Sc means that the effect of cilia on deposition will be more significant for larger, less diffusive particles, as well as for systems at lower temperatures, for which transport by diffusion is relatively slow.

The non-trivial relationship between E and Sp results from the flow patterns generated by cilia oscillating with different Sp. Figure 5 shows the period-averaged flow fields for various Sp. The flow fields are calculated using the period-averaged velocity of non-diffusive tracer particles. Due to symmetry, a slice x–y plane at the center of the cilia in the z-direction is given only for the bottom half of the channel from the middle plane between cilia in the x-direction and the left side of the cilia (Fig. 1).

In all cases presented in Fig. 5, oscillating cilia induce the secondary flows in the microchannel. However, among all these cases, $Sp = 3$ induces the fastest secondary flow with the velocity about an order of magnitude greater than for the other cases. We also find that the structure of flow is different for ciliated channels with $Sp = 2$ and 3 and with $Sp = 4$ and 5. When oscillated at $Sp = 2$ and 3, the cilia create a large circulating flow pattern (Fig. 5a, b) that transports the fluid upward near the cilia and downward in the center between neighboring cilia. On the other hand, when cilia oscillations are characterized by $Sp = 4$ and 5, the period-averaged flow includes multiple smaller vortices that locally transport fluid. These local circulations, however, are not sufficient to noticeably enhance the net transport of suspended nanoparticles, resulting in a relatively small E. Thus, we find that cilia with $Sp = 3$ are optimal for enhancing nanoparticle deposition.

To investigate the effect of cilia coverage density on deposition enhancement, simulations are performed in which we vary the spacing between cilia. The results are shown in Fig. 6. We find that E varies non-monotonically with cilia spacing, showing maximum enhancement at about $\delta x = 1.1\ L$. This optimal density of cilia coverage is independent of the Schmidt number. A similar optimal spacing has been previously reported for heat transport enhancement by tilted oscillating cilia (Mills et al. 2012), in which case the optimal spacing was related to the formation of flow structures in the ciliated layer. Smaller intercilial spacing prevents the development of circulatory flow currents, whereas excessive separation between neighboring cilia leaves parts of the fluid unagitated.

Finally, we investigate the effect of the magnitude of the cilia actuation force on deposition enhancement. As seen in Fig. 7, E increases with increasing driving force amplitude for $A < 12$. For larger values of A, E saturates or even slightly decreases. In other words, an additional increase in the oscillating force beyond $A = 12$ is unable to further enhance the deposition of nanoparticles. We can explain this by examining the displacement of oscillating cilia. We find that cilia displacement approaches a limiting cycle as the driving force is about 12. Further increase in the force magnitude essentially does not affect the cilium displacement and, therefore, has a weak effect on nanoparticle deposition.

We also find that cilia can exhibit transition from a two-dimensional to three-dimensional beating pattern when the oscillating force amplitude exceeds a critical value A_{cr} (Fig. 8). When driven by relatively small oscillatory forces, cilia beat in a periodic two-dimensional non-reciprocal pattern, as shown for $A = 6$ in Fig. 8a and b. However, when the driving force is increased to $A = 8$, the beating cilia exhibit a periodic three-dimensional pattern. The three-dimensional motion of cilia with $A = 8$ is further illustrated in Fig. 8c and d, showing a sequence of projections of the cilium centerline on the x–y and x–z planes,

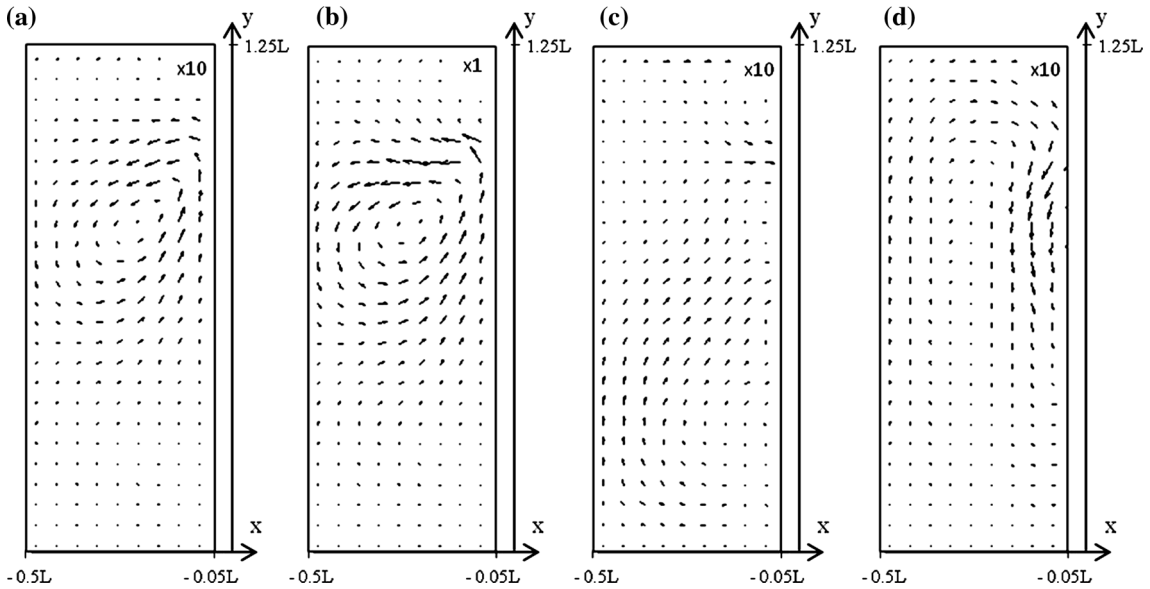

Fig. 5 Period-averaged velocity in the x–y (cilia motion) plane (see Fig. 1b) with $Sp = 1$, $\delta x/L = 1$, and **a** $Sp = 3$, **b** $Sp = 3$, **c** $Sp = 4$, **d** $Sp = 5$. For clarity, velocity magnitudes for $Sp = 3$, 4, and 5 are scaled up by a factor of 10 as compared with those for $Sp = 3$. The flow pattern for $Sp = 3$ has the most significant impact on nanoparticle deposition

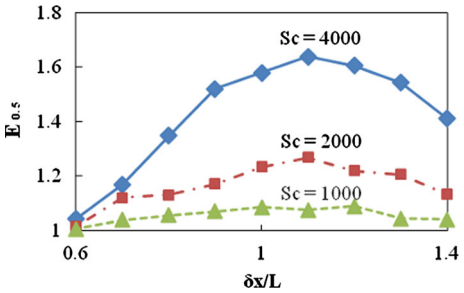

Fig. 6 Dependence of E at 50 % deposition on cilia spacing $\delta x/L$. The simulation parameters are $Sp = 3$, $A = 1$, and $\delta z = \delta x/2$

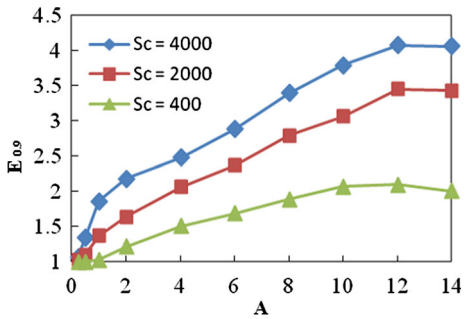

Fig. 7 Dependence of E at 90 % deposition on oscillation amplitude A for various Sc, $Sp = 3$, and $\delta x/L = 1$

respectively, during an oscillation period. Our simulations show that the critical amplitude of the oscillatory force causing the transition for $Sp = 3$ is $A_{cr} \approx 7$.

The three-dimensional bending of cilia is caused by a buckling instability (Guglielmini et al. 2012; Vogel and Stark 2012; Son et al. 2013). Buckling occurs when the oscillating force $A > A_{cr}$ bends the cilia to the side and then drives them in the opposite direction, as shown in Fig. 8e. Buckling causes cilium bending in the x–z plane, thereby inducing three-dimensional motion of the oscillating cilia. This behavior resembles Euler's buckling instability of columns. We can estimate the critical force leading to cilium buckling by considering an axially loaded long column with unsupported length of 0.75 L, which is approximately equal to the length of the horizontal section of cilia in our simulations at the onset of buckling. Replacing the oscillatory external force with a constant compressive force and using Euler's formula for the critical force for a column with fixed–free end conditions (Landau and Lifshitz 1970), we estimate the magnitude of the dimensionless force required to induce buckling to be approximately 1.5. This value is close to the instantaneous external force experienced by cilia at the onset of buckling, which is found in simulations to be approximately 4, indicating that the three-dimensional motion is indeed a result of cilium buckling during the beating cycle.

4 Summary

Using three-dimensional numerical simulations, we probe how arrays of oscillating synthetic cilia can be used to enhance the deposition of nanoparticles onto the walls of a microfluidic channel. The synthetic cilia are high-aspect-ratio elastic filaments that are actuated by a periodic force

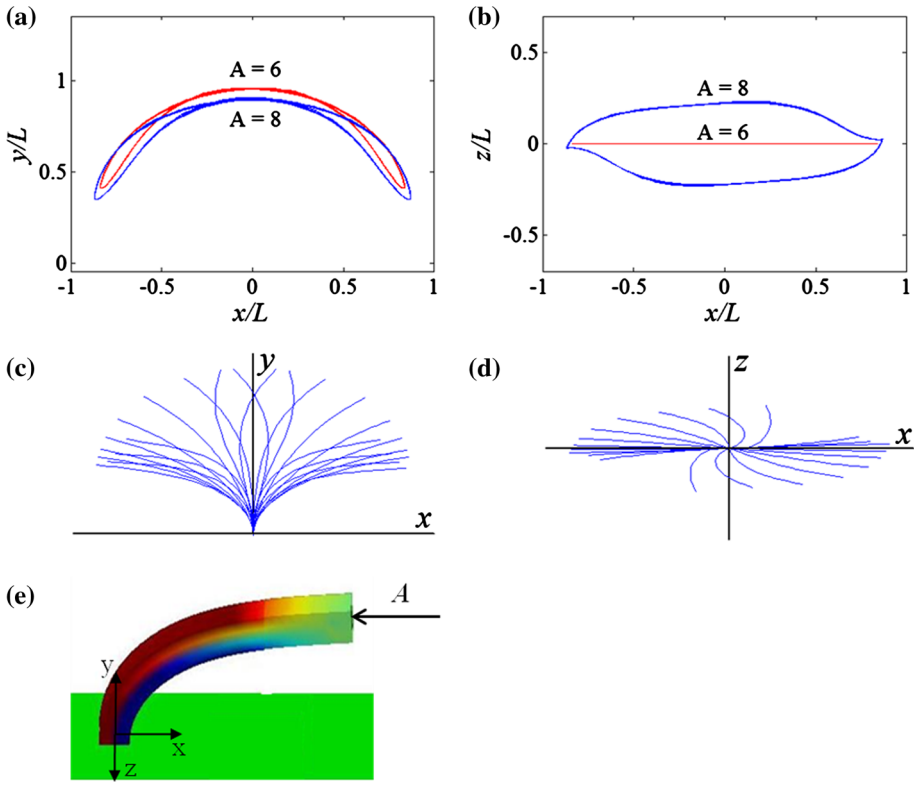

Fig. 8 Cilium tip trajectory for $Sp = 3$ and $\delta x/L = 1$ **a** in the x–y plane and **b** in the x–z plane. Cilia movement is two-dimensional when the driving force amplitude is $A = 6$, but becomes three-dimensional when the driving force amplitude is increased to $A = 8$. **c** and **d** show centerlines of cilia with $A = 8$ at different instants of cilia beating in the x–y and x–z planes, respectively. **e** Three-dimensional motion is a result of cilia buckling, due to a compressive force applied to the cilium end when it is bent over horizontally

applied to their free ends. We find that secondary flows created by beating cilia can significantly accelerate deposition and that this effect is more pronounced for larger particles and in systems with lower temperatures characterized by slower diffusion.

The fastest deposition is found for cilia oscillating at $Sp = 3$ and separated by a distance of about $\delta x = 1.1\ L$. In this case, cilia engage a substantial amount of fluid in an intensive circulatory motion that effectively convects nanoparticles toward the microchannel walls. Increasing the magnitude of the actuating force intensifies the secondary flow, thereby increasing the deposition rate. However, when the force amplitude exceeds $A = 12$, the cilia oscillation cycle saturates, and a further increase in driving force strength has only a minor effect on deposition.

Furthermore, our simulations reveal that large actuation forces cause the cilia to move in a three-dimensional periodic bending pattern. This three-dimensional motion arises due to cilia buckling taking place when filaments are bent horizontally.

The results of our study are useful for designing microfluidic devices in which actuated synthetic cilia are employed to enhance microscale transport processes. In particular, beating cilia can be utilized in microfluidic sensors to enhance their sensitivity by facilitating the deposition of particulates on sensory surfaces. Beating regimes creating convective flows are also relevant for applications in which rapid mixing at the microscale is required.

Researchers have proposed different synthetic cilia actuated by external magnetic and electrical forces and by self-oscillating chemical reactions taking place inside the filaments (Den Toonder and Onck 2013a). These synthetic cilia exhibit a wide range of sizes, mechanical properties, different actuation patterns, and beating frequencies. Here, we focus on regular arrays of identical cilia. However, the use of cilia arrays composed of filaments with different sizes, mechanics, and stimulus responses, as well as arrays of individually addressable filaments opens an elegant way to create locally actuated ciliated surfaces to precisely drive the fluid flows and deposit specific nanoparticles.

Finally, we note that although in our simulations we consider externally actuated synthetic cilia driven in a relatively simple stroke, the results shed additional light on the utility of cilia by biological organisms that employ cilia for transporting nutrition and feeding.

Acknowledgments Financial support from NSF (CBET-1256403) is gratefully acknowledged.

References

Alexeev A, Verberg R, Balazs AC (2005) Modeling the motion of microcapsules on compliant polymeric surfaces. Macromolecules 38:10244–10260

Alexeev A, Verberg R, Balazs AC (2006) Designing compliant substrates to regulate the motion of vesicles. Phys Rev Lett 96:148103

Alexeev A, Yeomans JM, Balazs AC (2008) Designing synthetic, pumping cilia that switch the flow direction in microchannels. Langmuir 24:12102–12106

Babataheri A, Roper M, Fermigier M, Du Roure O (2011) Tethered fleximags as artificial cilia. J Fluid Mech 678:5

Bird RB, Stewart WE, Lightfoot EN (2002) Transport phenomena. Wiley, New York

Bouzidi M, Firdaouss M, Lallemand P (2001) Momentum transfer of a Boltzmann-lattice fluid with boundaries. Phys Fluids 13:3452–3459

Brennen C, Winet H (1977) Fluid-mechanics of propulsion by cilia and flagella. Annu Rev Fluid Mech 9:339–398

Buxton GA, Care CM, Cleaver DJ (2001) A lattice spring model of heterogeneous materials with plasticity. Model Simul Mater Sci Eng 9:485–497

Dayal P, Kuksenok O, Bhattacharya A, Balazs AC (2012) Chemically-mediated communication in self-oscillating, biomimetic cilia. J Mater Chem 22:241–250

Den Toonder JMJ, Onck PR (2013a) Artificial cilia. RSC nanoscience & nanotechnology. RSC Publishing, Cambridge

Den Toonder JMJ, Onck PR (2013b) Microfluidic manipulation with artificial/bioinspired cilia. Trends Biotechnol 31:85–91

Evans BA, Shields AR, Carroll RL, Washburn S, Falvo MR, Superfine R (2007) Magnetically actuated nanorod arrays as biomimetic cilia. Nano Lett 7:1428–1434

Ghosh R, Buxton GA, Usta OB, Balazs AC, Alexeev A (2010) Designing oscillating cilia that capture or release microscopic particles. Langmuir 26:2963–2968

Guglielmini L, Kushwaha A, Shaqfeh ESG, Stone HA (2012) Buckling transitions of an elastic filament in a viscous stagnation point flow. Phys Fluids 24:123601

Keißner A, Brücker C (2012) Directional fluid transport along artificial ciliary surfaces with base-layer actuation of counter-rotating orbital beating patterns. Soft Matter 8:5342–5349

Khaderi SN, Craus CB, Hussong J, Schorr N, Belardi J, Westerweel J, Prucker O, Ruhe J, den Toonder JMJ, Onck PR (2011) Magnetically-actuated artificial cilia for microfluidic propulsion. Lab Chip 11:2002–2010

Ladd AJC, Verberg R (2001) Lattice-Boltzmann simulations of particle-fluid suspensions. J Stat Phys 104:1191–1251

Landau LD, Lifshitz EM (1970) Theory of elasticity. Course of theoretical physics, vol 7, 2d English edn. Pergamon Press, Oxford

Malvadkar NA, Hancock MJ, Sekeroglu K, Dressick WJ, Demirel MC (2010) An engineered anisotropic nanofilm with unidirectional wetting properties. Nat Mater 9:1023–1028

Marsaglia G, Tsang WW (2000) The ziggurat method for generating random variables. J Stat Softw 5:1–7

Masoud H, Alexeev A (2011a) Harnessing synthetic cilia to regulate motion of microparticles. Soft Matter 7:8702–8708

Masoud H, Alexeev A (2011b) Selective control of surface properties using hydrodynamic interactions. Chem Commun 47:472–474

Mills ZG, Aziz B, Alexeev A (2012) Beating synthetic cilia enhance heat transport in microfluidic channels. Soft Matter 8: 11508–11513

Mills ZG, Mao W, Alexeev A (2013) Mesoscale modeling: solving complex flows in biology and biotechnology. Trends Biotechnol 31:426–434

Oh K, Chung JH, Devasia S, Riley JJ (2009) Bio-mimetic silicone cilia for microfluidic manipulation. Lab Chip 9:1561–1566

Oh K, Smith B, Devasia S, Riley JJ, Chung JH (2010) Characterization of mixing performance for bio-mimetic silicone cilia. Microfluid Nanofluid 9:645–655

Pokroy B, Epstein AK, Persson-Gulda MCM, Aizenberg J (2009) Fabrication of bioinspired actuated nanostructures with arbitrary geometry and stiffness. Adv Mater 21:463–469

Purcell EM (1977) Life at low Reynolds number. Am J Phys 45:3–11

Riisgard HU, Larsen PS (2001) Minireview: ciliary filter feeding and bio-fluid mechanics—present understanding and unsolved problems. Limnol Oceanogr 46:882–891

Satir P, Christensen ST (2007) Overview of structure and function of mammalian cilia. Ann Rev Physiol 69:377–400

Semmler C, Alexeev A (2011) Designing structured surfaces that repel fluid-borne particles. Phys Rev E 84:066303

Shields AR, Fiser BL, Evans BA, Falvo MR, Washburn S, Superfine R (2010) Biomimetic cilia arrays generate simultaneous pumping and mixing regimes. Proc Natl Acad Sci USA 107: 15670–15675

Sleigh MA (1989) Adaptations of ciliary systems for the propulsion of water and mucus. Comp Biochem Physiol 94:359–364

Son K, Guasto JS, Stocker R (2013) Bacteria can exploit a flagellar buckling instability to change direction. Nat Phys 9:494–498

Succi S (2001) The lattice Boltzmann equation for fluid dynamics and beyond. Numerical mathematics and scientific computation. Oxford University Press, Oxford

Timonen JVI, Johans C, Kontturi KS, Walther A, Ikkala O, Ras RHA (2010) A facile template-free approach to magneto driven, multifunctional artificial cilia. ACS Appl Mater Interfaces 2:2226–2230

Tripathi A, Bhattacharya A, Balazs AC (2013) Size selectivity in artificial cilia–particle interactions: mimicking the behavior of suspension feeders. Langmuir 29:4616–4621

Tuckerman M, Berne BJ, Martyna GJ (1992) Reversible multiple time scale molecular-dynamics. J Chem Phys 97:1990–2001

Verberg R, Alexeev A, Balazs AC (2006) Modeling the release of nanoparticles from mobile microcapsules. J Chem Phys 125:224712

Verberg R, Dale AT, Kumar P, Alexeev A, Balazs AC (2007) Healing substrates with mobile, particle-filled microcapsules: designing a 'repair and go' system. J R Soc Interface 4:349–357

Vilfan M, Potočnik A, Kavčič B, Osterman N, Poberaj I, Vilfan A, Babič D (2010) Self-assembled artificial cilia. Proc Natl Acad Sci 107:1844–1847

Vogel R, Stark H (2012) Motor-driven bacterial flagella and buckling instabilities. Eur Phys J E 35:1–15

Wang EN, Bucaro MA, Taylor JA, Kolodner P, Aizenberg J, Krupenkin T (2009) Droplet mixing using electrically tunable superhydrophobic nanostructured surfaces. Microfluid Nanofluid 7:137–140

Wiggins CH, Riveline D, Ott A, Goldstein RE (1998) Trapping and wiggling: elastohydrodynamics of driven microfilaments. Biophys J 74:1043–1060